Supporting Information for

Synthesis, Properties, and OFET Characteristics of 5,5′-Di(2-azulenyl)-2,2′-bithiophene (DAzBT) and 2,5-Di(2-azulenyl)-thieno[3,2-*b*]thiophene (DAzTT)

Yuji Yamaguchi, Yukihiro Maruya, Hiroshi Katagiri*, Ken-ichi Nakayama, and Yoshihiro Ohba
Graduate School of Science and Engineering, Yamagata University, 4-3-16 Jonan, Yonezawa, Yamagata 992-8510, Japan

Contents

Experimental Section

General: All chemicals and solvents were reagent grade quality, obtained commercially and used without further purification except as noted. All reactions were performed in standard, dry glassware under an inert atmosphere of nitrogen. Column chromatography were performed using Kanto silica gel 60N, spherical neutral, 40–100 μm. Thin Layer Chromatography (TLC) were performed using pre-coated aluminium sheets covered with 0.20 mm silica gel with fluorescent indicator UV 254 nm. Melting points were determined with a Yanaco MP-500P apparatus. Nuclear magnetic resonance spectra were obtained on a JEOL JNM-ECX operating at 500 MHz for ^{1}H or 125 MHz for ^{13}C in deuterated chloroform with TMS as internal reference; chemical shifts (δ) are reported in parts per million. Elemental analyses were performed on Perkin Elmer 2400 series II CHNS/O elemental analyzer.

Physicochemical Studies: UV-vis spectra were measured on a Shimadzu UV-3150 UV-VIS-NIR spectrophotometer. Photoemission yield spectroscopy (PYS) spectra were measured on a RIKEN KEIKI AC-3. X-ray diffraction (XRD) was recorded on Rigaku Smartlab system. Thermal gravimetric analysis (TGA) was performed on a SII TG/DTA 6200. AFM images were recorded on Bruker Dimension Icon.

1. Synthesis

2-(2-Azulenyl)-5-chlorothiophene 3:

A mixture of $Pd(PPh_3)_4$ (155 mg, 0.134 mmol), 2-iodoazulene **1** (1.12 g, 4.41 mmol), 2-(5-chlorothiophene-2-yl)-5,5-dimethyl-[1,3,2]dioxaborinane **2** (1.22 g, 5.29 mmol), 2M $NaHCO_3$ aq. (4.5 ml) in toluene (9 ml) and EtOH (2.2 ml) was refluxed for 30 min under nitrogen atmosphere. After cooling to room temperature, the mixture was poured into water (100 ml) and extracted with chloroform. The organic phase was dried over Na_2SO_4 and concentrated under reduced pressure. The residue was purified by recrystallization from hexane/toluene to give **3** (786 mg, 73%).

Blue crystals; mp 213.0 °C; ^{1}H NMR (500 MHz, $CDCl_3$) δ 8.20 (d, J = 9.8 Hz, 2H), 7.49 (dd, J = 9.8, 9.8 Hz, 1H), 7.43 (s, 2H), 7.33 (d, J = 4.0 Hz, 1H), 7.15 (dd, J = 9.8, 9.8 Hz, 2H), 6.94 (d, J = 4.0 Hz, 1H); ^{13}C NMR (125 MHz, $CDCl_3$) δ 142.25, 141.29, 139.72, 136.41, 135.72, 130.78, 127.54, 124.72, 124.33, 113.46; Anal. Calcd for $C_{14}H_9ClS$: C, 68.71; H, 3.71; S, 13.10. Found: C, 68.69; H, 3.64; S, 13.29.

5,5′-Di(2-azulenyl)-2,2′-bithiophene (DAzBT):

To a solution of PPh_3 (3.25 g, 12.4 mmol) in dry DMF (20 ml), $NiCl_2$ (400 mg, 3.09 mmol) and zinc powder (250 mg, 3.82 mmol) were added, and the resulting mixture was stirred at 50 °C under nitrogen atmosphere for 1 hour. 2-(2-Azulenyl)-5-chlorothiophene **3** was added to the mixture, and it

was then stirred at 50 °C under nitrogen atmosphere for 1 hour. After cooling to room temperature, the mixture was poured into 5% EDTA aq. (200 ml) and the resulted precipitate was collected by filtration. The residue was washed with methanol, hexane, and then toluene, and the precipitate was purified by gradient sublimation to give **DAzBT** (381 mg, 60%).

Dark green crystals; mp >300 °C; Anal. Calcd for $C_{28}H_{18}S_2$: C, 80.34; H, 4.33; S, 15.32. Found: C, 80.41; H, 4.34; S, 15.34.

2,5-Di(2-azulenyl)-thieno[3,2-*b*]thiophene (DAzTT):

A mixture of $Pd(PPh_3)_4$ (107 mg, 0.093 mmol), 2-iodoazulene **1** (800 mg, 3.15 mmol), 2,5-bis(4,4,5,5-tetramethyl-1,3,2-dioxaborolan-2-yl)-thieno[3,2-*b*]thiophene **4** (590 mg, 1.50 mmol), 2M $NaHCO_3$ aq. (3 ml) in toluene (6 ml) and EtOH (1.5 ml) was refluxed for 45 min under nitrogen atmosphere. After mixture was poured into water (100 ml) and the resulted precipitate was collected by filtration. The residue was washed with ethanol, hexane, and then chloroform, and the precipitate was purified by gradient sublimation to give **DAzTT** (233 mg, 40%).

Dark green crystals; mp >300 °C; Anal. Calcd for $C_{26}H_{16}S_2$: C, 79.55; H, 4.11; S, 16.34. Found: C, 79.63; H, 4.11; S, 16.21.

2. NMR Spectra

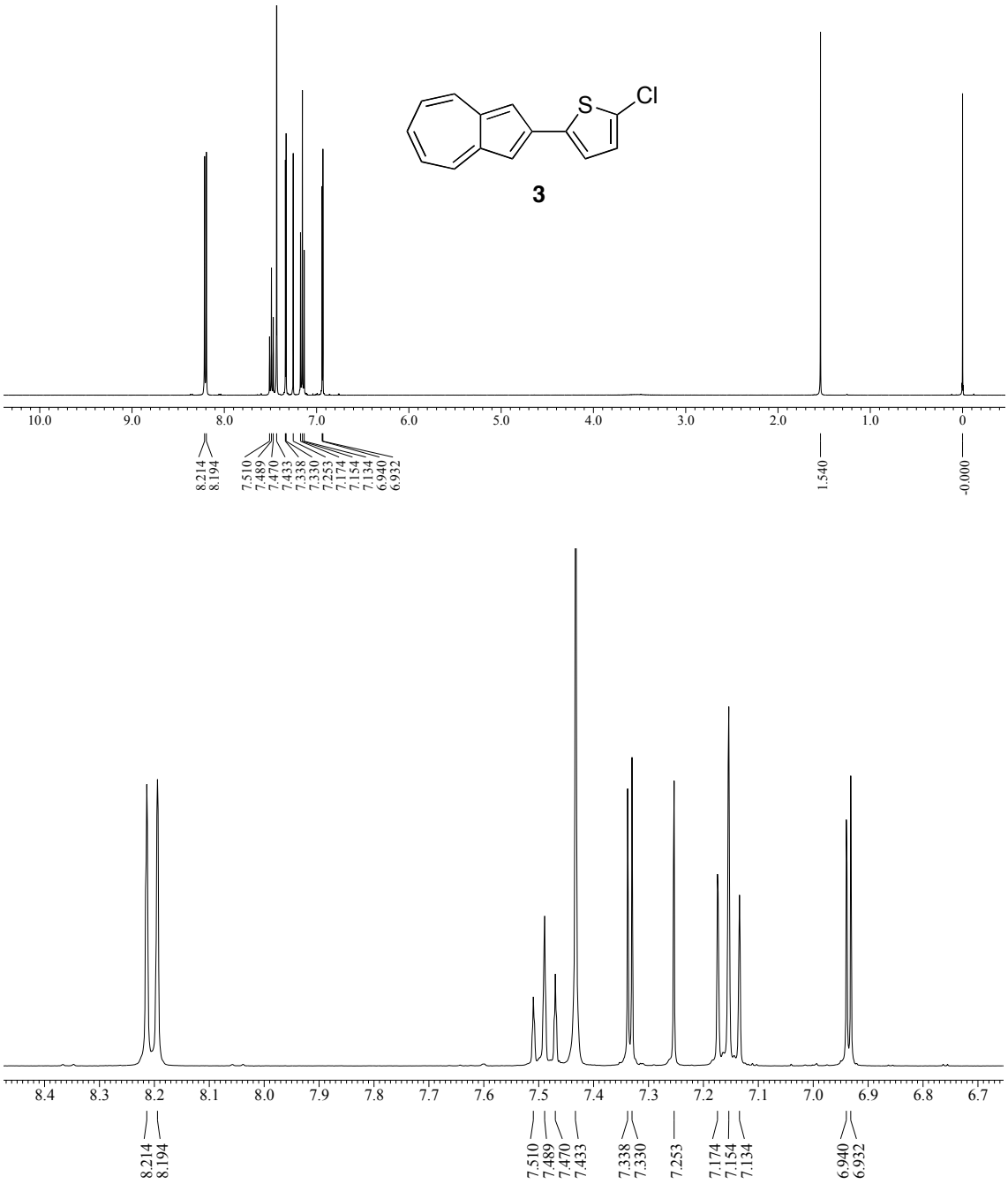

Figure S1. ^{1}H NMR spectrum of **3** (500 MHz, $CDCl_3$, 25 °C).

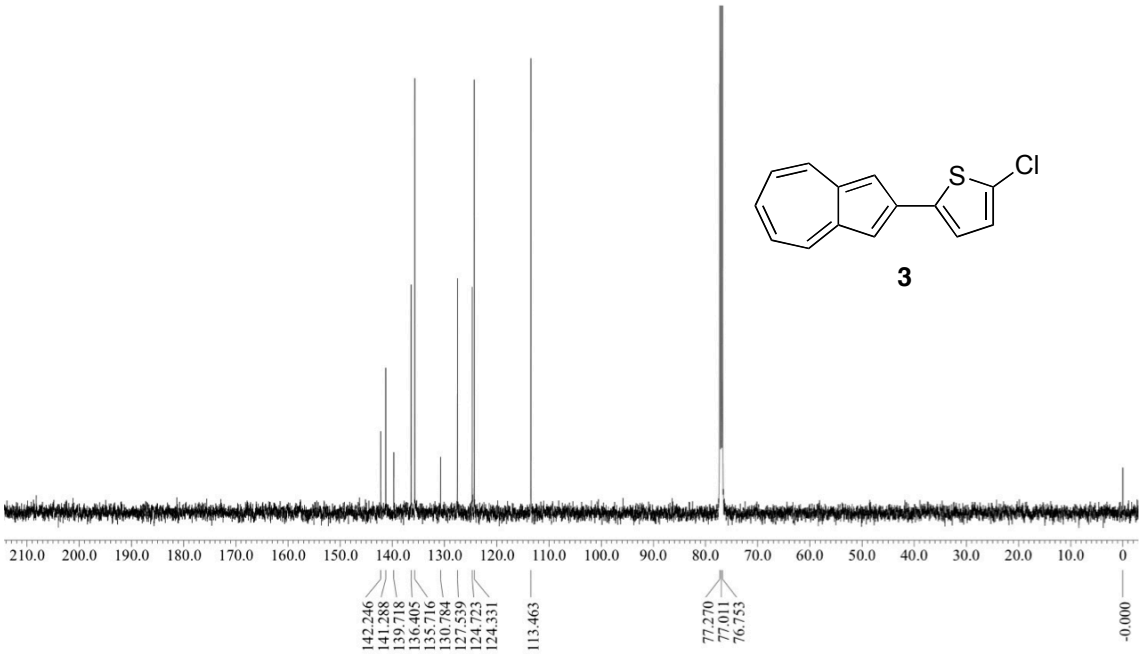

Figure S2. ^{13}C NMR spectrum of **3** (125 MHz, $CDCl_3$, 25 °C).

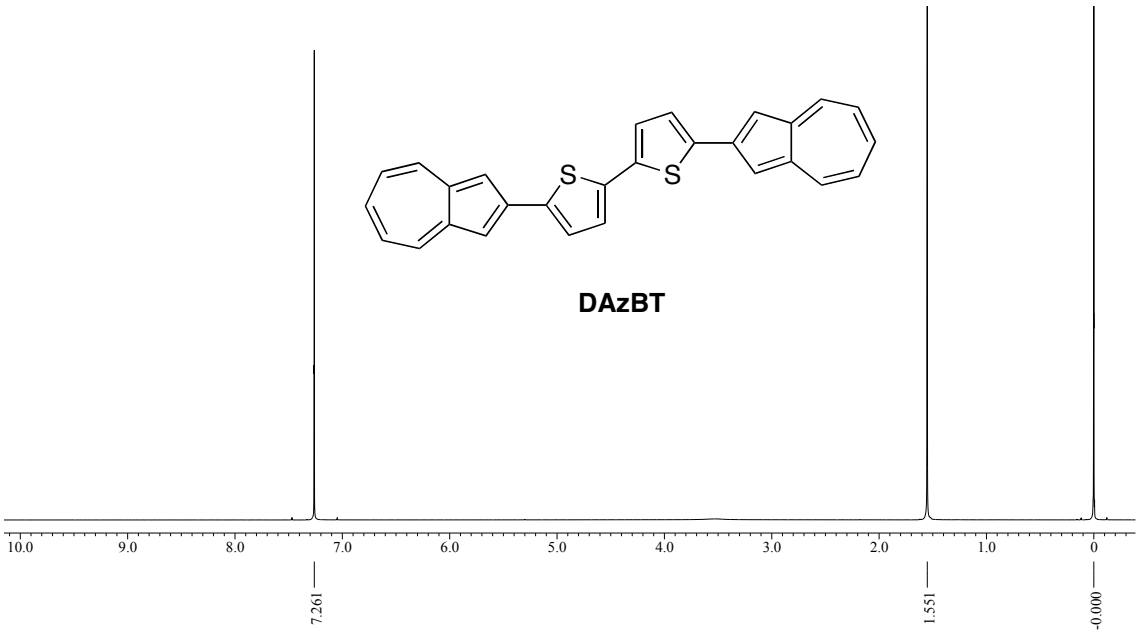

Figure S3. ^{1}H NMR spectrum of **DAzBT** (500 MHz, $CDCl_3$, 25 °C).

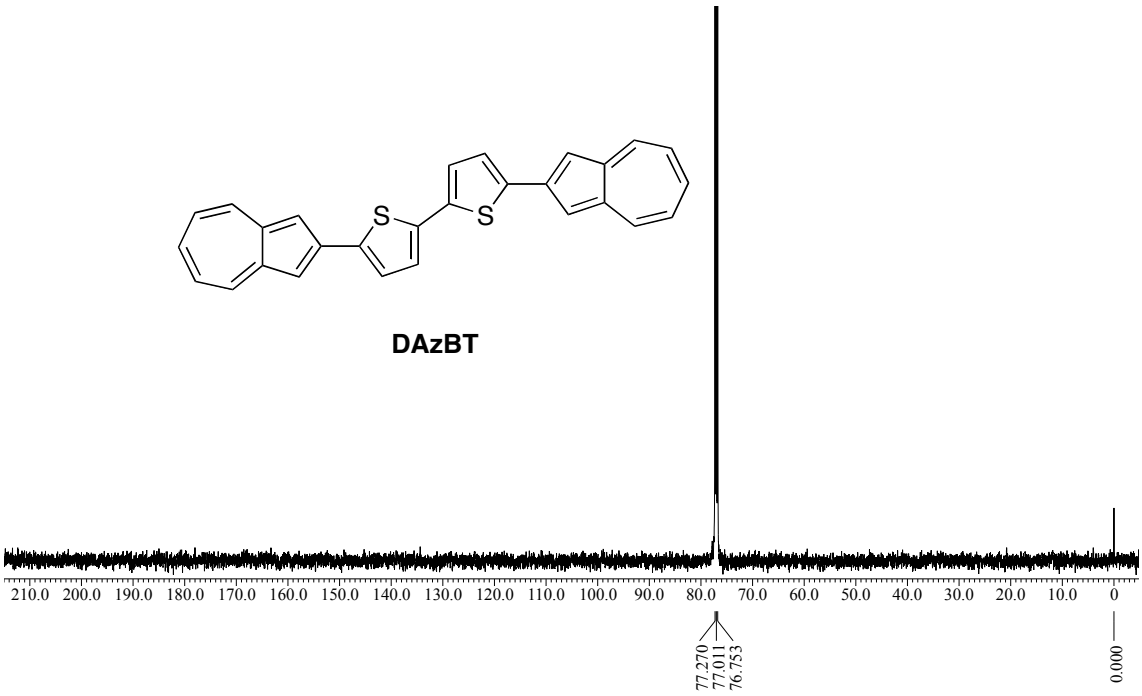

Figure S4. ^{13}C NMR spectrum of **DAzBT** (125 MHz, $CDCl_3$, 25 °C).

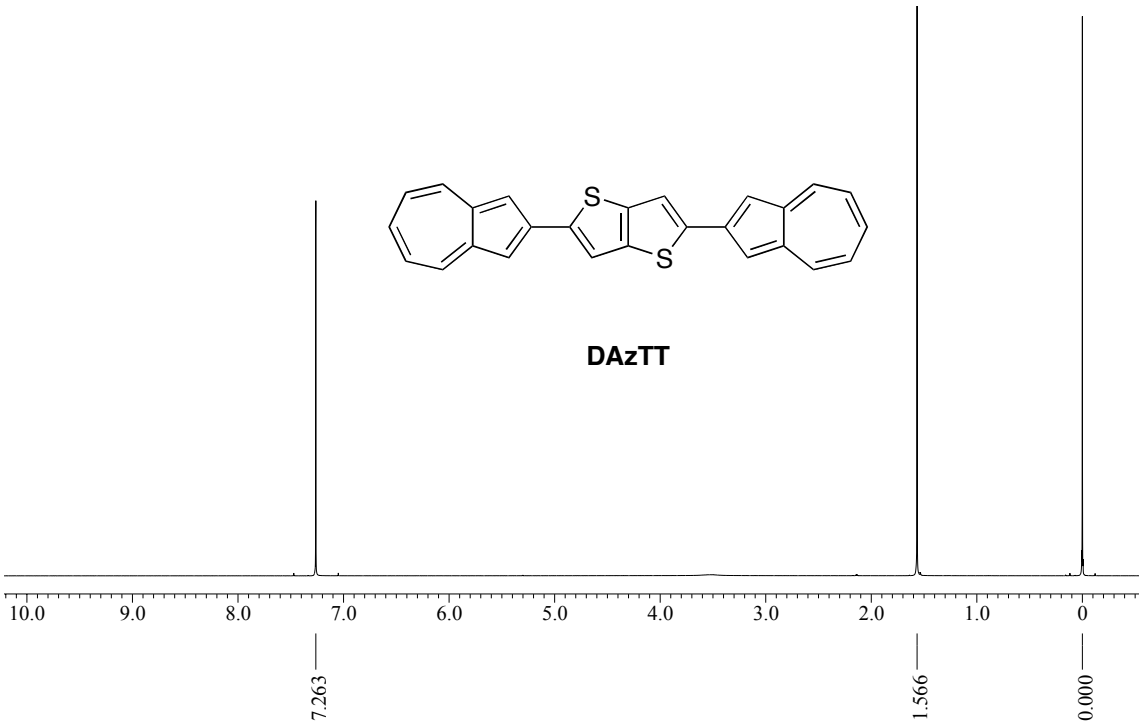

Figure S5. ^{1}H NMR spectrum of **DAzTT** (500 MHz, $CDCl_3$, 25 °C).

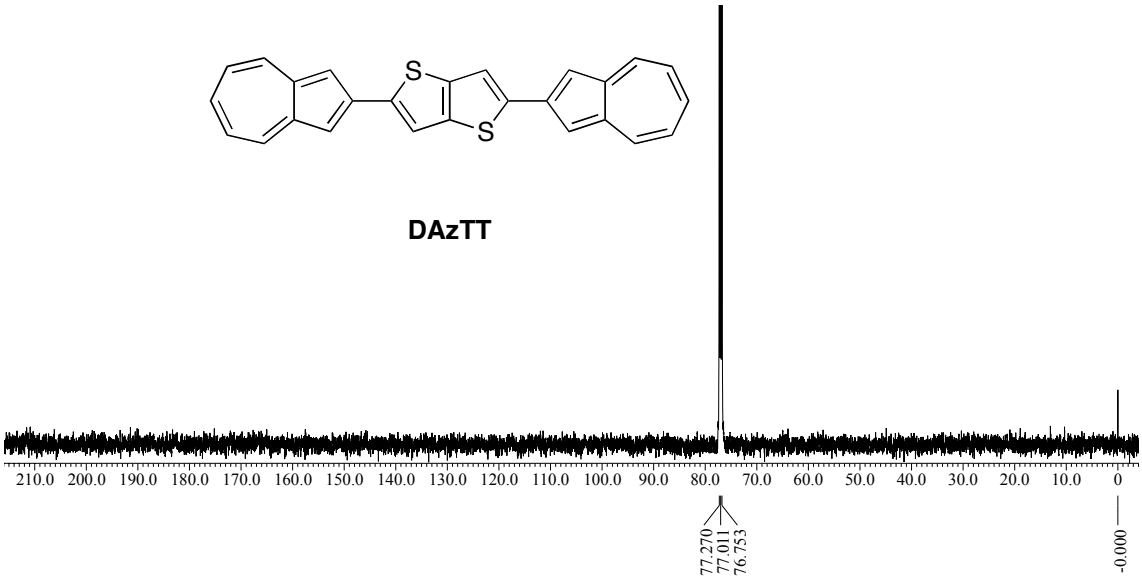

Figure S6. ^{13}C NMR spectrum of **DAzTT** (125 MHz, $CDCl_3$, 25 °C).

3. X-ray Crystallographic Structure Determination for DAzBT (Figure S7 and Table S1).

X-Ray diffraction data for **DAzBT** was collected on a Rigaku Saturn 724 CCD diffractometer with Mo-Kα radiation (λ = 0.71075 Å) at 103 K. Single crystals of **DAzBT** [$C_{28}H_{18}S_2$, Mw = 418.57] suitable for X-ray analysis were grown by slow gradient sublimation, and a dark green crystal with dimensions 0.70 × 0.10 × 0.05 mm was selected for intensity measurements. The unit cell was monoclinic with the space group *P*21/a. Lattice constants with $Z = 2$, $r_{calcd} = 1.416$ g cm^{-3}, μ(Mo-Kα) = 2.85 cm^{-1}, $F(000) = 436$, 2θmax = 55.24° were a = 6.055(6), b = 7.542(8), c = 21.60(2) Å, α = 90°, β = 95.65(2)°, γ = 90°, and V = 981.6(18) Å^3. A total of 11402 reflections were collected, of which 2267 reflections were independent ($R_{int} = 0.0999$). Structure was refined to final $R1 = 0.0849$ for 1539 data [$I>2\sigma(I)$] with 136 parameters and $wR2 = 0.2321$ for all data, GOF = 1.087, and residual electron density max./min. = 0.565/–0.338 eÅ^{-3}. The ORTEP drawing is shown in Figure S3, and the crystal data and structure refinement are listed in Table S1.

Data collection, cell refinement, and data reduction were carried out using the CrystalClear-SM software[1]. The structure was solved by direct methods using the program SHELXS-97[2] and refined by full-matrix least squares methods on F^2 using SHELXL-97[3]. All materials for publication were prepared by Yadokari-XG 2009 software[4]. All non-hydrogen atoms were refined anisotropically. The positions of all hydrogen atoms were calculated geometrically and refined as a riding model.

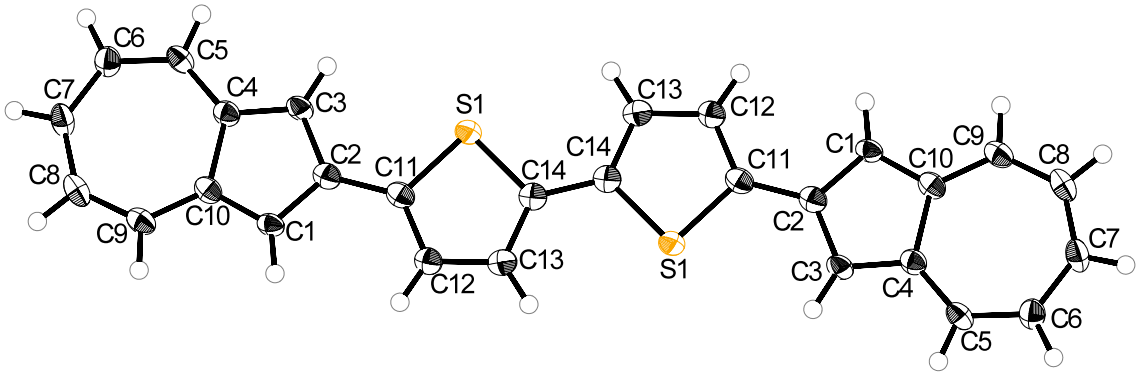

Figure S7. ORTEP diagram of **DAzBT** with thermal ellipsoids at 50% probability.

Table S1. Crystal data and structure refinement for **DAzBT**.

Empirical formula	C28 H18 S2	
Formula weight	418.57	
Temperature	103 K	
Wavelength	0.71075 Å	
Crystal system	monoclinic	
Space group	P 21 /a	
Unit cell dimensions	a = 6.055(6) Å	$\alpha = 90°$
	b = 7.542(8) Å	$\beta = 95.65(2)°$
	c = 21.60(2) Å	$\gamma = 90°$
Volume	981.6(18) $Å^3$	
Z	2	
Density (calculated)	1.416 g/cm^3	
Absorption coefficient	0.285 mm^{-1}	
F(000)	436	
Crystal size	0.70 × 0.10 × 0.05 mm	
Theta range for data collection	3.30 to 27.62°	
Index ranges	–7<=h<=7, –9<=k<=9, –28<=l<=28	
Reflections collected	11402	
Independent reflections	2267 [R(int) = 0.0999]	
Completeness to theta = 27.62°	99.3%	
Absorption correction	Semi-empirical from equivalents	
Max. and min. transmission	1.0000 and 0.7829	
Refinement method	Full-matrix least-squares on F^2	
Data / restraints / parameters	2267 / 0 / 136	
Goodness-of-fit on F^2	1.087	
Final R indices [I>2sigma(I)]	R1 = 0.0849, wR2 = 0.2043	
R indices (all data)	R1 = 0.1223, wR2 = 0.2321	
Largest diff. peak and hole	0.565 and –0.338 $e.Å^{-3}$	

4. X-ray Crystallographic Structure Determination for DAzTT (Figure S8 and Table S2).

X-Ray diffraction data for **DAzTT** was collected on a Rigaku Saturn 724 CCD diffractometer with Mo-Kα radiation (λ = 0.71075 Å) at 93 K. Single crystals of **DAzTT** [$C_{26}H_{16}S_2$, Mw =392.54] suitable for X-ray analysis were grown by slow gradient sublimation, and a dark green crystal with dimensions 0.20 × 0.15 × 0.01 mm was selected for intensity measurements. The unit cell was triclinic with the space group *P*-1. Lattice constants with Z = 2, r_{calcd} = 1.440 g cm^{-3}, μ(Mo-Kα) = 3.03 cm^{-1}, F(000) = 408, 2θmax = 54.86° were a = 5.866(5), b = 7.860(6), c = 20.022(15) Å, α = 81.85(2)°, β = 82.430(18)°, γ = 87.35(2)°, and V = 905.5(12) Å^3. A total of 12390 reflections were collected, of which 4088 reflections were independent (R_{int} = 0.0655). Structure was refined to final $R1$ = 0.0677 for 4088 data [$I>2\sigma(I)$] with 289 parameters and $wR2$ = 0.1809 for all data, GOF = 1.066, and residual electron density max./min. = 0.444/–0.398 eÅ^{-3}. The ORTEP drawing is shown in Figure S4, and the crystal data and structure refinement are listed in Table S2.

Data collection, cell refinement, and data reduction were carried out using the CrystalClear-SM software[1]. The structure was solved by direct methods using the program SHELXS-97[2] and refined by full-matrix least squares methods on F^2 using SHELXL-97[3]. All materials for publication were prepared by Yadokari-XG 2009 software[4]. All non-hydrogen atoms were refined anisotropically. The positions of all hydrogen atoms were calculated geometrically and refined as a riding model.

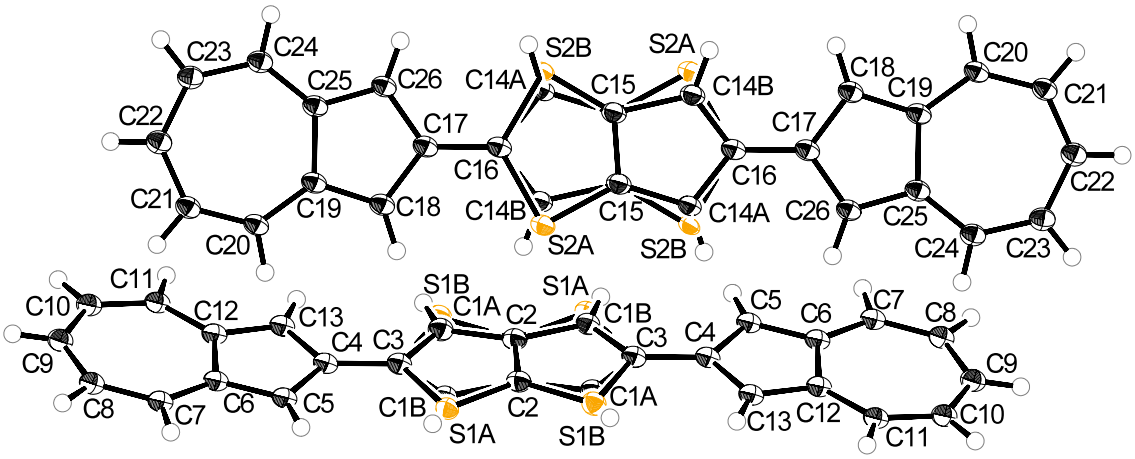

Figure S8. ORTEP diagram of **DAzTT** with thermal ellipsoids at 50% probability.

Table S2. Crystal data and structure refinement for **DAzTT**.

Empirical formula	C26 H16 S2	
Formula weight	392.54	
Temperature	93 K	
Wavelength	0.71075 Å	
Crystal system	triclinic	
Space group	P -1	
Unit cell dimensions	a = 5.866(5) Å	α = 81.85(2)°
	b = 7.860(6) Å	β = 82.430(18)°
	c = 20.022(15) Å	γ = 87.35(2)°
Volume	905.5(12) $Å^3$	
Z	2	
Density (calculated)	1.440 g/cm^3	
Absorption coefficient	0.303 mm^{-1}	
F(000)	408	
Crystal size	0.20 × 0.15 × 0.01 mm	
Theta range for data collection	3.11 to 27.43°	
Index ranges	−7<=h<=7, −10<=k<=10, −25<=l<=25	
Reflections collected	12390	
Independent reflections	4088 [R(int) = 0.0655]	
Completeness to theta =27.43°	99.0%	
Absorption correction	Semi-empirical from equivalents	
Max. and min. transmission	1.0000 and 0.8747	
Refinement method	Full-matrix least-squares on F^2	
Data / restraints / parameters	4088 / 216 / 289	
Goodness-of-fit on F^2	1.066	
Final R indices [I>2sigma(I)]	R1 = 0.0677, wR2 = 0.1502	
R indices (all data)	R1 = 0.1133, wR2 = 0.1809	
Largest diff. peak and hole	0.444 and –0.398 $e.Å^{-3}$	

5. MO Calculations

All calculations were performed using Gaussian 09 program[5]. The geometries were optimized at the B3LYP/6-31G(d) level without any symmetry constraints. The time-dependent density functional theory (TD-DFT) calculations were conducted at the B3LYP/6-31G(d) level of theory.

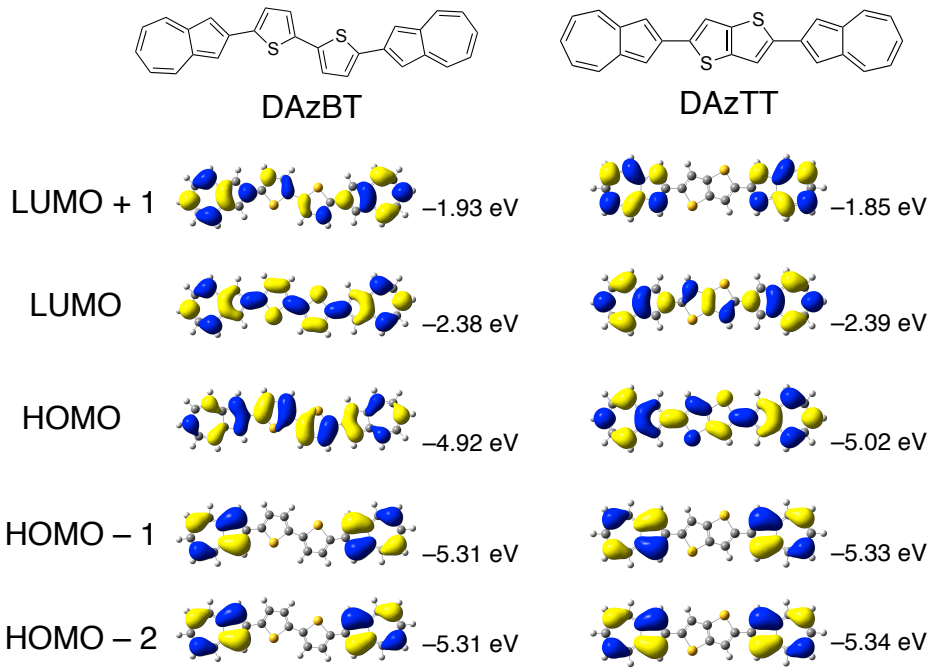

Figure S9. Molecular orbitals of **DAzBT** and **DAzTT**.

DAzBT:

E(RB3LYP) = –1874.12718092 a.u.

Imaginary Freq = 0

Excited State	1:	Triplet	1.3606 eV	911.24 nm	f=0.0000
Excited State	2:	Triplet	1.7620 eV	703.64 nm	f=0.0000
Excited State	3:	Triplet	1.9460 eV	637.14 nm	f=0.0000
Excited State	4:	Triplet	1.9462 eV	637.04 nm	f=0.0000
Excited State	5:	Singlet	2.2747 eV	545.07 nm	f=0.0960
HOMO–2 → LUMO		0.59156			
HOMO–1 → LUMO+1		0.31581			
HOMO → LUMO		0.18409			
Excited State	6:	Singlet	2.2780 eV	544.28 nm	f=0.0000
HOMO–2 → LUMO+1		0.32065			

HOMO–1 → LUMO		0.61588			
Excited State	7:	Triplet	2.3522 eV	527.10 nm	f=0.0000
Excited State	8:	Singlet	2.3723 eV	522.63 nm	f=1.6678
HOMO–2 → LUMO		–0.17284			
HOMO → LUMO		0.68138			
Excited State	9:	Triplet	2.5179 eV	492.40 nm	f=0.0000
Excited State	10:	Triplet	2.6693 eV	464.49 nm	f=0.0000

Table S3. Optimized geometry of **DAzBT**

Atom	X	Y	Z
C	0.343580	–9.801855	–0.162756
C	1.519509	–9.045554	–0.162745
C	1.667648	–7.656646	–0.162807
C	–0.990649	–9.378143	–0.162834
C	0.682224	–6.668795	–0.162898
C	–1.495713	–8.077746	–0.162923
C	0.802024	–6.864984	–0.162956
H	0.486615	–10.881212	–0.162695
H	2.445738	–9.616198	–0.162677
H	2.693889	–7.290023	–0.162780
H	–1.735309	–10.171257	–0.162825
H	–2.582135	–7.991673	–0.162975
C	0.903756	–5.287559	–0.162957
H	1.878626	–4.813892	–0.162944
C	–0.343978	–4.618050	–0.163050
C	–1.376499	–5.591550	–0.163048
H	–2.440569	–5.389275	–0.163098
C	–0.550732	–3.187602	–0.163133
C	–1.743044	–2.486628	–0.163323
S	0.800850	–2.065387	–0.162987
C	–1.585613	–1.083872	–0.163369
H	–2.709939	–2.977227	–0.163445
C	–0.264539	–0.670446	–0.163213
H	–2.418903	–0.389052	–0.163540
C	0.264539	0.670446	–0.163213
C	1.585613	1.083872	–0.163369

S	–0.800850	2.065387	–0.162987
C	1.743044	2.486628	–0.163323
H	2.418903	0.389052	–0.163540
C	0.550732	3.187602	–0.163133
H	2.709939	2.977227	–0.163445
C	0.343978	4.618050	–0.163050
C	–0.903756	5.287559	–0.162957
C	1.376499	5.591550	–0.163048
C	–0.682224	6.668795	–0.162898
H	–1.878626	4.813892	–0.162944
C	0.802024	6.864984	–0.162956
H	2.440569	5.389275	–0.163098
C	–1.667648	7.656646	–0.162807
C	1.495713	8.077746	–0.162923
C	–1.519509	9.045554	–0.162745
H	–2.693889	7.290023	–0.162780
C	0.990649	9.378143	–0.162834
H	2.582135	7.991673	–0.162975
C	–0.343580	9.801855	–0.162756
H	–2.445738	9.616198	–0.162677
H	1.735309	10.171257	–0.162825
H	–0.486615	10.881212	–0.162695

DAzTT:

E(RB3LYP) = –1796.71233492 a.u.

Imaginary Freq = 0

Excited State	1:	Triplet	1.4198 eV	873.27 nm	f=0.0000
Excited State	2:	Triplet	1.8728 eV	662.02 nm	f=0.0000
Excited State	3:	Triplet	1.9400 eV	639.09 nm	f=0.0000
Excited State	4:	Triplet	1.9493 eV	636.05 nm	f=0.0000
Excited State	5:	Singlet	2.2724 eV	545.62 nm	f=0.0208
HOMO–2 → LUMO+1		–0.28202			
HOMO–1 → LUMO		0.62923			
HOMO → LUMO		0.09987			
Excited State	6:	Singlet	2.2808 eV	543.60 nm	f=0.0000
HOMO–2 → LUMO		0.63330			
HOMO–1 → LUMO+1		–0.28884			
Excited State	7:	Triplet	2.4747 eV	501.01 nm	f=0.0000
Excited State	8:	Singlet	2.5016 eV	495.62 nm	f=1.6476
HOMO → LUMO		0.69595			
Excited State	9:	Triplet	2.5512 eV	485.99 nm	f=0.0000
Excited State	10:	Triplet	2.8705 eV	431.92 nm	f=0.0000

Table S4. Optimized geometry of **DAzTT**

Atom	X	Y	Z
C	–2.317601	0.000268	–0.155076
C	–1.457618	–1.083036	–0.155075
S	–1.425756	1.534109	–0.155075
H	–1.803643	–2.109675	–0.155079
C	–0.100076	–0.691231	–0.155073
C	0.100076	0.691231	–0.155073
C	1.457618	1.083036	–0.155075
C	2.317601	–0.000268	–0.155076
S	1.425756	–1.534109	–0.155075
H	1.803643	2.109675	–0.155079
C	–3.763248	–0.011137	–0.155083
C	–4.610340	1.123348	–0.155103
C	–4.572926	–1.176785	–0.155070

C	–5.943584	0.699158	–0.155105
H	–4.287084	2.157825	–0.155120
C	–5.917321	–0.797537	–0.155082
H	–4.215747	–2.199339	–0.155048
C	–7.066354	1.527290	–0.155125
C	–7.013828	–1.663626	–0.155074
C	–8.418081	1.174834	–0.155127
H	–6.855889	2.596517	–0.155140
C	–8.374567	–1.356989	–0.155086
H	–6.767542	–2.725246	–0.155056
C	–8.991441	–0.100159	–0.155110
H	–9.119747	2.006189	–0.155144
H	–9.048564	–2.210940	–0.155076
H	–10.080066	–0.118850	–0.155115
C	3.763248	0.011137	–0.155083
C	4.610340	–1.123348	–0.155103
C	4.572926	1.176785	–0.155070
C	5.943584	–0.699158	–0.155105
H	4.287084	–2.157825	–0.155120
C	5.917321	0.797537	–0.155082
H	4.215747	2.199339	–0.155048
C	7.066354	–1.527290	–0.155125
C	7.013828	1.663626	–0.155074
C	8.418081	–1.174834	–0.155127
H	6.855889	–2.596517	–0.155140
C	8.374567	1.356989	–0.155086
H	6.767542	2.725246	–0.155056
C	8.991441	0.100159	–0.155110
H	9.119747	–2.006189	–0.155144
H	9.048564	2.210940	–0.155076
H	10.080066	0.118850	–0.155115

6. Photoemission Yield Spectroscopy in Air

The IP levels of **DAzBT** and **DAzTT** were determined by Photoemission yield spectroscopy (PYS). Thin films were prepared by vapor deposition to ITO substrate with 60nm of thickness. Intensity of UV-light was 10.0 nW.

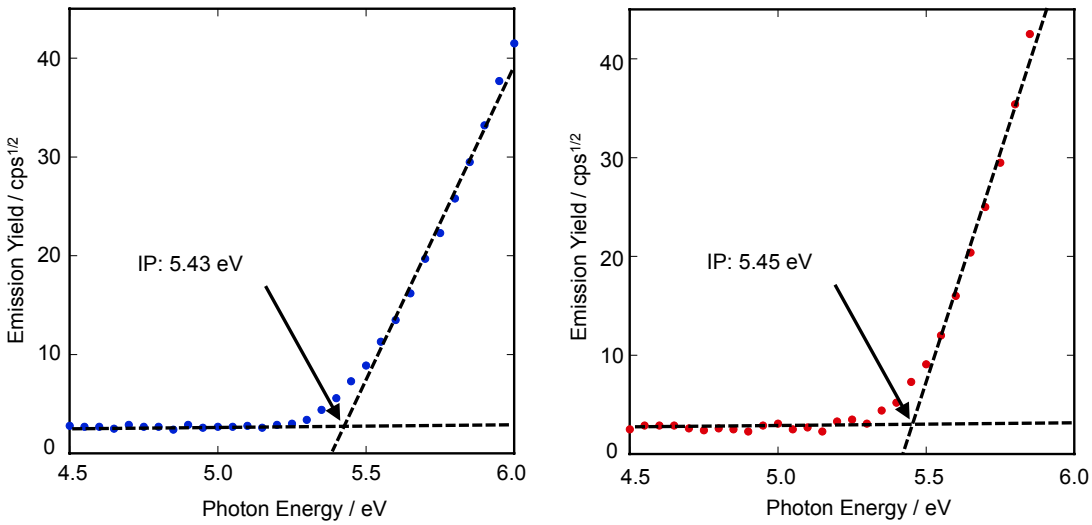

Figure S10. Photoemission yield spectroscopy in air of **DAzBT** (left) and **DAzTT** (right).

7. Device Fabrications and Evaluations

The field-effect mobility of **DAzBT** and **DAzTT** were measured using top-contact thin-film field-effect transistor (FET) geometry. The heavily doped n^+-Si (100) substrate functions as the gate electrode. A 300 nm thickness SiO_2 dielectric layer with a capacitance of 11.8 $nFcm^{-2}$ was thermally grown on the gate substrate. A thin film (60 nm thick) of **DAzBT** and **DAzTT** as the active layer was vacuum-deposited on the bare or HMDS treated Si/SiO_2 substrates maintained at room temperature at a rate of 0.9–1.8 $Å s^{-1}$ under a pressure of ~2×10^{-5} Pa. On top of the organic thin film, gold films (30 nm) as drain and source electrodes were deposited through a shadow mask. For a typical device, the drain-source channel length (L) and width (W) are 50 μm and 5.5 mm, respectively. The characteristics of the OFET devices were measured at room temperature under nitrogen with an Agilent Technologies 4155C Semiconductor Parameter Analyzer, operated by an Interactive Characterization Software (ICS), version 3.6.0. Field-effect mobility (μ_{FET}) was calculated in the saturation regime ($V_D = -100$ V) of the I_D using the following equation,

$$I_D = (WC_i / 2L)\, \mu_{FET}\, (V_G - V_{Th})^2$$

where C_i is the capacitance of the SiO_2 insulator, and V_G and V_{Th} are the gate and threshold voltages, respectively. Current on/off ratio (I_{on}/I_{off}) was determined from the I_D at $V_G = 0$ V (I_{off}) and $V_G = -100$ V (I_{on}).

8. AFM images of Active-layer on Substrate

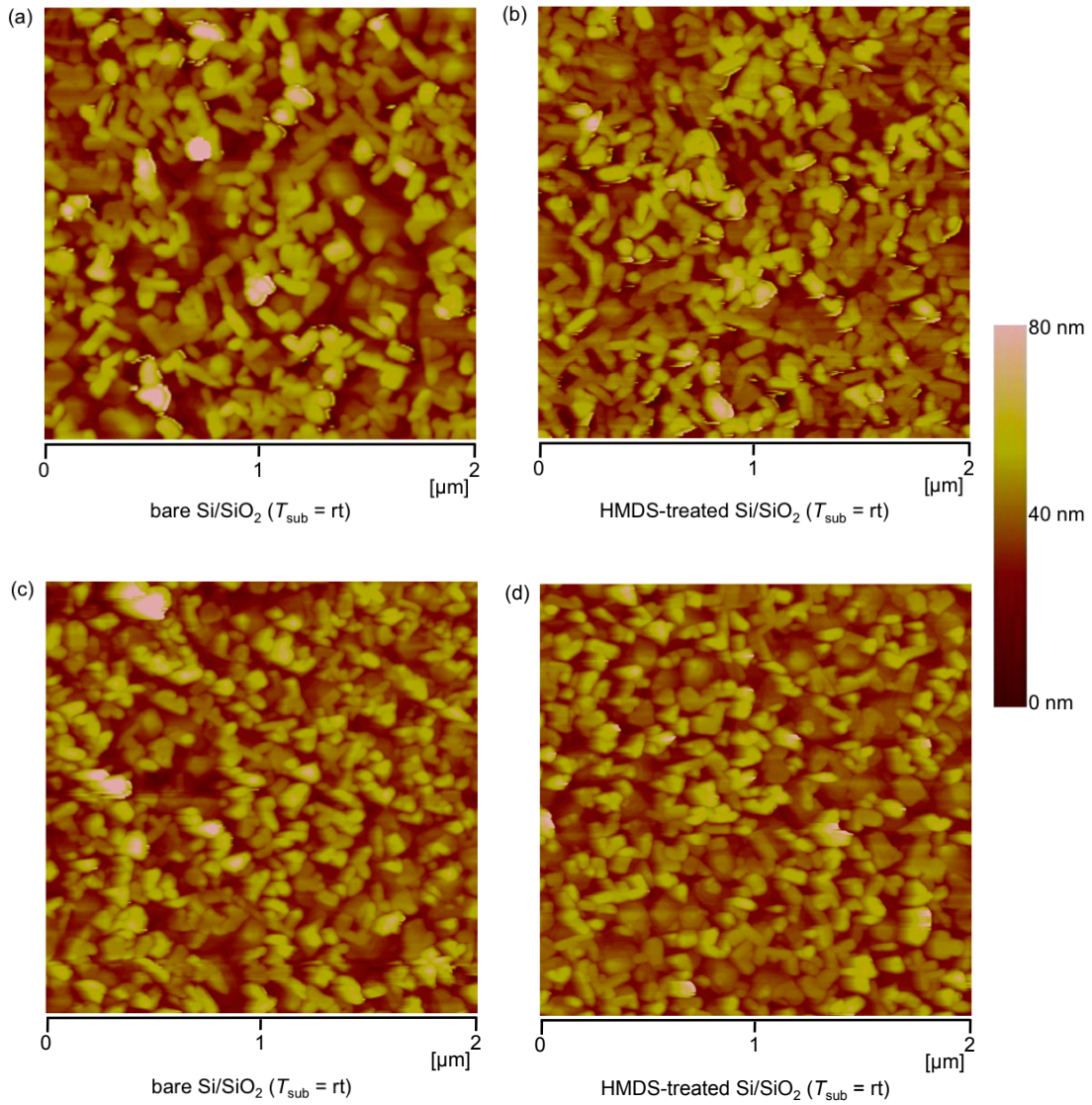

Figure S11. AFM images of **DAzBT** (a, b) and **DAzTT** (c, d).

9. TGA analysis

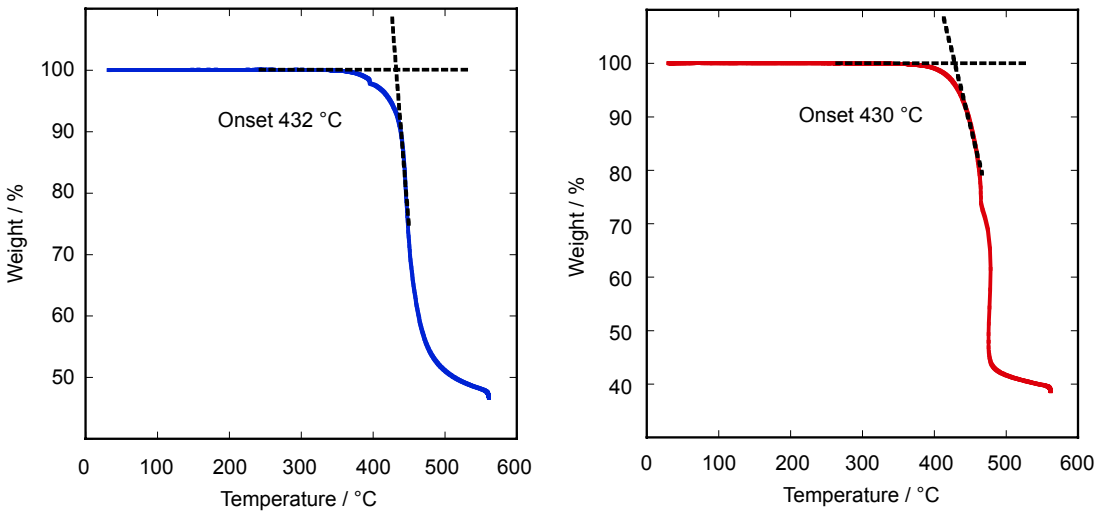

Figure S12. TGA measurements for **DAzBT** (left) and **DAzTT** (right). The heating rate is 10 °C/min under N_2.

10. References

[1] CrystalClear: Rigaku Corporation, Tokyo, Japan, **2005**.

[2] SHELXS-97: Sheldrick, G. M. Program for the Solution of Crystal Structures; *Acta Crystallogr. A* **2008**, *64*, 112–122.

[3] SHELXL-97: Sheldrick, G. M. Program for the Refinement of Crystal Structures; *Acta Crystallogr. A* **2008**, *64*, 112–122.

[4] (a) Yadokari-XG: Wakita, K. Software for crystal Structure Analyses, **2001**. (b) Yadokari-XG 2009: Kabuto, C.; Akine, S.; Nemoto, T.; Kwon, E. Release of Software for Crystal Structure Analyses; *J. Cryst. Soc. Jpn.* **2009**, *51*, 218–224.

[5] Gaussian 09, Revision C.01: Frisch, M. J.; Trucks, G. W.; Schlegel, H. B.; Scuseria, G. E.; Robb, M. A.; Cheeseman, J. R.; Scalmani, G.; Barone, V.; Mennucci, B.; Petersson, G. A.; Nakatsuji, H.; Caricato, M.; Li, X.; Hratchian, H. P.; Izmaylov, A. F.; Bloino, J.; Zheng, G.; Sonnenberg, J. L.; Hada, M.; Ehara, M.; Toyota, K.; Fukuda, R.; Hasegawa, J.; Ishida, M.; Nakajima, T.; Honda, Y.; Kitao, O.; Nakai, H.; Vreven, T.; Montgomery, Jr., J. A.; Peralta, J. E.; Ogliaro, F.; Bearpark, M.; Heyd, J. J.; Brothers, E.; Kudin, K. N.; Staroverov, V. N.; Kobayashi, R.; Normand, J.; Raghavachari, K.; Rendell, A.; Burant, J. C.; Iyengar, S. S.; Tomasi, J.; Cossi, M.; Rega, N.; Millam, N. J.; Klene, M.; Knox, J. E.; Cross, J. B.; Bakken, V.; Adamo, C.; Jaramillo, J.; Gomperts, R.; Stratmann, R. E.; Yazyev, O.; Austin, A. J.; Cammi, R.; Pomelli, C.; Ochterski, J. W.; Martin, R. L.; Morokuma, K.; Zakrzewski, V. G.; Voth, G. A.; Salvador, P.; Dannenberg, J. J.; Dapprich, S.; Daniels, A. D.; Farkas, Ö.; Foresman, J. B.; Ortiz, J. V.; Cioslowski, J.; Fox, D. J. Gaussian, Inc., Wallingford CT, **2009**.